AGU PUBLICATIONS

Radio Science

RESEARCH ARTICLE
10.1002/2017RS006381

Special Section:
Special Issue of the 2016 URSI Commission B International Symposium on Electromagnetic Theory

Key Points:
- In this paper, we investigate the potentials of light trapping in complex-shaped open plasmonic resonators (meta-atoms)
- It is demonstrated that such nanostructures may support embedded light states perfectly screened by volume plasmons
- It is shown that the embedded eigenstates can be efficiently pumped by a plane wave when the meta-atom core has a nonlinear response

Correspondence to:
M. G. Silveirinha,
mario.silveirinha@co.it.pt

Citation:
Silva, S., Morgado, T. A., & Silveirinha, M. G. (2018). Discrete light spectrum of complex-shaped meta-atoms. *Radio Science*, *53*. https://doi.org/10.1002/2017RS006381

Received 1 JUN 2017
Accepted 21 DEC 2017
Accepted article online 4 JAN 2018

Discrete Light Spectrum of Complex-Shaped Meta-atoms

Solange Silva[1], Tiago A. Morgado[1], and Mário G. Silveirinha[1,2]

[1]Instituto de Telecomunicações, Department of Electrical Engineering, University of Coimbra, Coimbra, Portugal, [2]Instituto Superior Técnico, University of Lisbon, Lisbon, Portugal

Abstract We investigate the potentials of open plasmonic resonators (meta-atoms) with different shapes in the context of light trapping. Consistent with the theory of Silveirinha (2014), it is found that in some conditions complex-shaped dielectric cavities may support discrete light states screened by volume plasmons that in the limit of vanishing material loss have an infinite lifetime. The embedded eigenstates can be efficiently pumped with a plane wave excitation when the meta-atom core has a nonlinear response, such that the trapped light energy is precisely quantized.

1. Introduction

The natural modes of oscillation of a physical system can be usually split into two categories: the bound modes—which form the discrete spectrum—and the extended modes—which form the continuous spectrum. Usually, the discrete and the continuous spectra do not overlap. For example, in the hydrogen atom the allowed electron energy levels are split into two disjoint subsets: the discrete negative energies (bound states) and the continuous positive energies (free-electron states). The discrete spectrum is invariably associated with spatially localized states that are square integrable and hence normalizable. On the other hand, the continuous spectrum is associated with delocalized (extended) states that are not square-integrable. The emergence of a spatially localized state in a regime wherein the natural modes are inherently delocalized is contrary to common sense and may seem a priori impossible because of the markedly different nature of these states. For example, in electronic systems it is counterintuitive to have a bound state at the same energy level for which the system supports free-electron states. Surprisingly, it was shown by von Neumann and Wigner in 1929 that bound states embedded in the continuum (embedded eigenstates) are really allowed within the framework of the usual wave theories (Stillinger & Herrick, 1975; Von Neumann & Wigner, 1929), and the concept of an electronic state with "positive energy" was even experimentally verified in the context of semiconductor heterostructures (Capasso et al., 1992).

Notably, in recent years there has been a considerable interest in the emergence of embedded eigenstates in photonic platforms (Hsu et al., 2013, 2016; Lee et al., 2012; Marinica et al., 2008; Molina et al., 2012; Plotnik et al., 2011). In particular, it has been shown that open material structures (e.g., standing in free space) with tailored geometries may support spatially localized stationary light oscillations with a square integrable electromagnetic field distribution, notwithstanding that at the same oscillation frequency the system also supports infinitely many spatially extended modes (belonging to the continuous spectrum) (Hsu et al., 2013; Lee et al., 2012; Marinica et al., 2008; Molina et al., 2012; Plotnik et al., 2011). Here we note that in photonic platforms formed by material inclusions standing in free space, a localized photonic state is always embedded in the radiation continuum and hence is an "embedded eigenstate." Moreover, it is highlighted that the emergence of embedded eigenstates in open (optically transparent) material structures is rather surprising because usually light escapes from any open region due to the radiation leakage. Until recently, all the known configurations to localize light in the radiation continuum with transparent materials required unbounded (infinitely extended) material structures (Hsu et al., 2013; Lee et al., 2012; Marinica et al., 2008; Molina et al., 2012; Plotnik et al., 2011), which in practice has limited interest. Any deviation from the ideal situation leads to a perturbed localized eigenstate with a finite lifetime.

In a recent series of works (Hrebikova et al., 2015; Lannebère & Silveirinha, 2015; Silveirinha, 2014), we developed a different paradigm to implement open material structures with a discrete light spectrum. It was shown that volume plasmons, that is, charge density oscillations in an electron gas, give the opportunity to confine light in a *spatially bounded* open optical cavity in such a manner that in ideal conditions the oscillation lifetime can be infinitely large (Hrebikova et al., 2015; Lannebère & Silveirinha, 2015; Liberal & Engheta, 2016a; Monticone & Alù, 2014; Silveirinha, 2014). Moreover, in Lannebère and Silveirinha (2015), we devised a

mechanism to pump the oscillations of the embedded eigenstate in a core-shell cavity and ensure at the same time that the trapped light energy has a precise value. In other words, the energy of the trapped light state is precisely quantized. Because of this property and due to the obvious analogies with electronic systems, the core-shell resonator is designated as "optical meta-atom." The key idea of the "meta-atom" concept is to exploit nonlinear effects to squeeze the wavelength of the incoming light into the core region until it reaches a very precise value for which the plasmonic shell blocks the trapped radiation from exiting the meta-atom (Lannebère & Silveirinha, 2015).

The objective of the present work is to explore alternative two-dimensional (2-D) meta-atom configurations and demonstrate that optical cavities with arbitrary complex shapes can support embedded eigenstates similar to those studied in Hrebikova et al. (2015), Lannebère and Silveirinha (2015), Monticone and Alù (2014), and Silveirinha (2014) for spherical core-shell geometries. Moreover, we investigate in detail realistic relaxation mechanisms of the meta-atom in the trapped regime, such as the leakage due to the conversion of light into higher-order harmonics.

This article is organized as follows. In section 2, we outline different possible cross-sectional geometries for the meta-atom and derive the conditions under which the meta-atom supports embedded eigenstates. In section 3, we analyze the electromagnetic response of the meta-atom in the linear regime. In section 4, the nonlinear response of the meta-atom and the quantization of the trapped light energy are investigated. The conclusions are drawn in section 5.

2. Embedded Eigenstates in Two-Dimensional Cavities

We consider a generic 2-D core-shell nanostructure of arbitrary shape (Figure 1) with a dielectric core with relative permittivity ε_1 and a shell with a plasma-type response in the frequency regime of interest. Specifically, it is assumed that the permittivity of the shell has a Drude-type dispersion $\varepsilon_2(\omega) = 1 - \omega_p^2/[\omega(\omega + i\omega_c)]$, where ω_p is the plasma frequency and ω_c is the collision frequency. The materials are nonmagnetic ($\mu = \mu_0$), and the meta-atom stands in free space. Figure 1 depicts a generic geometry of the structure, being implicit that the core-shell structure is invariant to translations along the z direction. It is also assumed that the fields are polarized in such a manner that $\mathbf{H} = H_z\hat{\mathbf{z}}$ and $\mathbf{E} = E_x\hat{\mathbf{x}} + E_y\hat{\mathbf{y}}$ (transverse magnetic (TM) polarization) and that the wave propagation is in the xoy plane with $\partial/\partial z = 0$. For now, it is supposed that the response of the involved materials is linear, but later we will allow the core to be characterized by a Kerr-type nonlinearity.

The embedded eigenstates may emerge in the regime wherein the shell supports volume plasmon oscillations, that is, when the permittivity of the shell vanishes, $\varepsilon_2(\omega_p) = 0$ (Silveirinha, 2014). Volume plasmons are nonradiative natural oscillations of an electron gas, which in some circumstances may hybridize with the radiation fields and in this manner perfectly screen the radiation in the core region (Silveirinha, 2014). From a purely electromagnetic point of view, this effect can be explained by the fact that a material with $\varepsilon = 0$ can behave as perfect magnetic conductor (PMC) for TM-polarized waves, which corresponds to an opaque boundary (Alù et al., 2007). Specifically, for TM-polarized waves, an $\varepsilon = 0$ material mimics precisely a PMC, except for incident waves that impinge on the material along the normal direction (Alù et al., 2007). For normal incidence, it is possible to have an energy flow through an ε-near-zero material (ENZ) due to an evanescent-type near-field tunneling effect (Engheta, 2013; Silveirinha & Engheta, 2006, 2009). Thus, the embedded eigenstates can occur at the frequency $\omega = \omega_p$ in the limit of vanishing material loss ($\omega_c \to 0$ with ε_1 real-valued).

Having a shell with $\varepsilon_2 = 0$ is a necessary but not a sufficient condition to trap light in the core-shell resonator. Indeed, there is an additional requirement: the geometry and the material parameters of the core region need to be such that $\omega = \omega_p$ is coincident with one of the natural oscillation frequencies ω_m^{PMC} (m = 1, 2, …) of the equivalent PMC cavity (Silveirinha, 2014):

$$\omega_p = \omega_m^{PMC} \tag{1}$$

for some m. In the system under study, the modes of the equivalent PMC cavity are solutions of a Dirichlet boundary value problem:

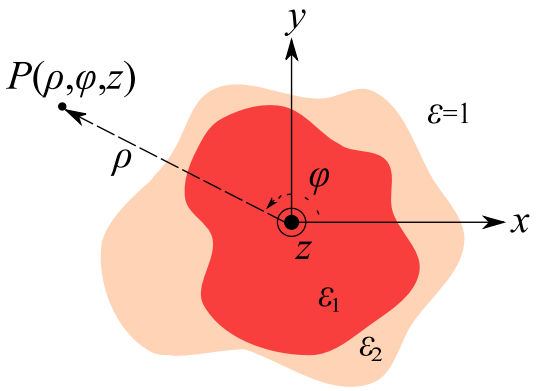

Figure 1. Generic geometry of the 2-D core-shell meta-atom (top view).

$$\nabla\cdot\left(\frac{1}{\varepsilon}\nabla H_z\right)+\frac{\omega^2}{c^2}H_z=0, \qquad \text{in the core region,} \tag{2a}$$

$$H_z=0, \qquad \text{at the core boundary.} \tag{2b}$$

Furthermore, in order that the field in the shell can have a purely electrostatic nature (volume plasmon mode), only the cavity modes with $\oint_{\text{core boundary}} \mathbf{E}\cdot\mathbf{dl}=0$ are allowed. Equivalently, because of Faraday's law, it is necessary that

$$\iint_{\text{core}} H_z dx dy=0. \tag{2c}$$

In the following subsections, we illustrate the outlined ideas for different geometries of the meta-atom. We would like to highlight that a few recent works have explored similar concepts to demonstrate that zero-index materials can be used to realize geometry-invariant cavities (Liberal & Engheta, 2016a, 2016b; Liberal, Mahmoud, & Engheta, 2016).

2.1. Circular Cross-Section Geometry

In the first example, the meta-atom has a circular cross section such that the core has radius R_1 and the shell has radius R_2. In this case, the eigenmodes of the equivalent PMC cavity (with a PMC wall placed at $\rho=R_1$) are the solutions of equation (2a):

$$H_z=H_0 e^{in\varphi}\begin{cases} J_{|n|}\left(\frac{\omega}{c}\sqrt{\varepsilon_1}\rho\right), & \rho<R_1 \\ 0, & \text{otherwise}\end{cases}, \tag{3}$$

where H_0 is a normalization constant and J_n is the Bessel function of the first kind and order n. Imposing the boundary condition (2b), it is found that H_z must vanish at $\rho=R_1$, which implies that for $\omega=\omega_p$,

$$J_{|n|}\left(\frac{\omega_p}{c}\sqrt{\varepsilon_1}R_1\right)=0. \tag{4}$$

This condition is satisfied only for well-defined values of the inner radius R_1 and of the core permittivity ε_1. Importantly, the embedded eigenmodes only occur for a nonzero azimuthal quantum number $n\neq 0$ ($\partial/\partial\varphi\neq 0$), so that condition (2c) can be satisfied. From a different perspective, for $n=0$ the electromagnetic fields are constant over the ENZ shell boundary ($\partial/\partial\varphi=0$). Hence, waves with $n=0$ impinge along the normal direction on the ENZ material interface so that the shell is penetrable by these waves. Thus, the ENZ shell behaves as a PMC wall only for TM-polarized waves with $\partial/\partial\varphi\neq 0$. As an example, for waves associated with the lowest-order positive mode $n=1$ (dipole mode), the first zero of $J_1(u)$ occurs for $u\approx 3.83$, and this gives the opportunity to have an embedded eigenmode with infinite lifetime for $R_1=R_{1,0}\equiv 3.83\frac{c}{\sqrt{\varepsilon_1}\omega_p}$ at $\omega=\omega_p$.

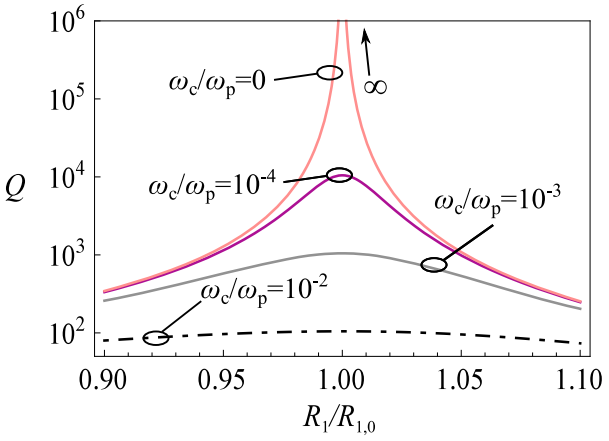

Figure 2. Quality factor as a function of $R_1/R_{1,0}$ for different values of the material loss in the cylindrical meta-atom shell and for the $n=1$ mode.

The electric field of a trapped mode in the core is calculated with the usual formulas $E_\rho=\frac{1}{-i\omega\varepsilon_1}\frac{1}{\rho}\partial_\varphi H_z$ and $E_\varphi=\frac{1}{i\omega\varepsilon_1}\partial_\rho H_z$, with H_z satisfying equation (3). On the other hand, the electric field in the shell must be a solution of the Laplace equation and thereby is of the form $\mathbf{E}=-\nabla\phi$ with $\phi=(A_1\rho^{|n|}+A_2\rho^{-|n|})e^{in\varphi}$. Taking into account that the tangential (azimuthal) electric field vanishes at the shell-air boundary and is continuous at the shell-core boundary, it is simple to prove that the electric potential satisfies

$$\phi=\eta_1 H_0 J'_{|n|}(k_1R_1)R_1\frac{1}{n}\frac{(\rho/R_2)^{|n|}-(\rho/R_2)^{-|n|}}{(R_1/R_2)^{|n|}-(R_1/R_2)^{-|n|}}e^{in\varphi}, \quad R_1<\rho<R_2. \tag{5}$$

Thus, the electromagnetic fields in the shell remain finite in the limiting case $\varepsilon_2=\varepsilon_2'+i\varepsilon_2''\to 0$, and there are no singularities in this limit.

In general, if the material loss is nonzero or if the core radius is detuned, the decay time becomes finite, and the corresponding oscillation frequency has an imaginary part: $\omega_r = \omega' + i\omega''$ with $\omega'' < 0$. This complex resonant frequency can be found by considering solutions of the wave equation of the form

$$H_z = H_0 e^{in\varphi} \begin{cases} a_n J_{|n|}(k_1\rho), & \rho < R_1 \\ b_n J_{|n|}(k_2\rho) + c_n Y_{|n|}(k_2\rho), & R_1 < \rho < R_2 \\ d_n H^{(1)}_{|n|}(k_0\rho), & \rho > R_2 \end{cases}, \tag{6}$$

where $k_0 = \omega/c$, $k_1 = k_0\sqrt{\varepsilon_1}$, $k_2 = k_0\sqrt{\varepsilon_2}$, Y_n is the Bessel function of the second kind and order n, and $H^{(1)}_n$ is the Hankel function of the first kind and order n. The coefficients a_n, b_n, c_n, and d_n must be such that H_z and $\frac{1}{\varepsilon}\frac{\partial H_z}{\partial \rho}$ are continuous functions of ρ at $\rho = R_1$ and $\rho = R_2$. This yields the following homogeneous linear system:

$$\begin{bmatrix} J_{|n|}(k_1R_1) & -J_{|n|}(k_2R_1) & -Y_{|n|}(k_2R_1) & 0 \\ 0 & -J_{|n|}(k_2R_2) & -Y_{|n|}(k_2R_2) & H^{(1)}_{|n|}(k_0R_2) \\ \frac{k_1}{\varepsilon_1}J'_{|n|}(k_1R_1) & -\frac{k_2}{\varepsilon_2}J'_{|n|}(k_2R_1) & -\frac{k_2}{\varepsilon_2}Y'_{|n|}(k_2R_1) & 0 \\ 0 & -\frac{k_2}{\varepsilon_2}J'_{|n|}(k_2R_2) & -\frac{k_2}{\varepsilon_2}Y'_{|n|}(k_2R_2) & k_0H^{(1)\prime}_{|n|}(k_0R_2) \end{bmatrix} \begin{bmatrix} a_n \\ b_n \\ c_n \\ d_n \end{bmatrix} = \begin{bmatrix} 0 \\ 0 \\ 0 \\ 0 \end{bmatrix}, \tag{7}$$

which has a nontrivial solution only when ω is such that the determinant of the matrix vanishes. The quality factor of the natural mode of oscillation is given by $Q = \omega'/(-2\omega'')$ and corresponds roughly to the ratio of the lifetime (τ_{ph}) and the period of oscillation (T): $Q/2\pi = \tau_{ph}/T$ (Silveirinha, 2014).

To illustrate the discussion, we consider the case wherein $R_2 = 1.1R_1$ and the meta-atom core is filled with air ($\varepsilon_1 = 1$). Figure 2 shows the calculated quality factor of the meta-atom as a function of the core radius $R_1/R_{1,0}$ and for different values of the shell material loss (i.e., different values of the normalized collision frequency ω_c/ω_p). As seen in Figure 2, in the ideal case wherein the collision frequency vanishes and the core radius is tuned so that $R_1/R_{1,0} = 1$, the quality factor diverges to infinity $Q = \infty$, which corresponds to an embedded eigenvalue with infinite lifetime. When the effect of material loss is considered or the core radius is detuned ($R_1 \neq R_{1,0}$), the quality factor and the oscillation lifetime become finite. Different from conventional dielectric resonators (e.g., whispering gallery cavities), the quality factor can be rather large even for subwavelength meta-atoms. In practice, the maximum quality factor is determined by the ENZ material loss. Similar to the theory of Silveirinha (2014) for a spherical cavity, it can be checked that when $R_1/R_{1,0} = 1$, the quality factor is $Q \approx \omega_p/\omega_c$ and hence is determined by the lifetime of the volume plasmons in the ENZ shell. It was shown in Silveirinha (2014) that possible spatial dispersion effects in the ENZ material response do not affect the peak value of Q, leading only to a slight reduction of the optimal value of the core radius.

In the shell region the magnetic field is of the form $H_z = e^{in\varphi}f_n(k_2\rho)$, and hence, it is possible to introduce a transverse impedance given by

$$\frac{E_\varphi}{H_z} \equiv Z_n^{TM} = \frac{k_2}{i\omega\varepsilon_0\varepsilon_2}\frac{f'_n(k_2\rho)}{f_n(k_2\rho)} = -i\eta_2\frac{f'_n(k_2\rho)}{f_n(k_2\rho)}, \tag{8}$$

where $\eta_2 = \eta_0/\sqrt{\varepsilon_2}$ is the impedance of the shell and f_n is some linear combination of Bessel functions of order n. It can be checked that in the limit $k_2\rho \to 0$ and for $n \geq 1$, $\frac{f'_n(k_2\rho)}{f_n(k_2\rho)} \sim \frac{1}{k_2\rho}$. Thus, the transverse impedance diverges, $Z_n^{TM} \to \infty$, in the limit wherein $\varepsilon_2 \to 0$. This confirms that the ENZ shell really behaves as a PMC for TM-polarized modes with $\partial/\partial\varphi \neq 0$. Quite differently, for modes with $n = 0$ the transverse impedance is finite in the ENZ limit. For example, if $f_0 = J_0(k_2\rho)$, it can be verified that when $\varepsilon_2 \to 0$, the impedance satisfies $Z_0^{TM} = i\eta_2 k_2\rho/2 = i\eta_0 k_0\rho/2$ and is therefore finite. Thus, the ENZ shell is generally penetrable by waves with $\partial/\partial\varphi = 0$ consistent with the discussion in the beginning of the subsection. It can also be verified that the transverse impedance of transverse electric (TE) waves (with electric field along the z direction and magnetic field in the xoy plane) is finite in the ENZ limit. Thus, the ENZ shell mimics the PMC response only for a specific wave polarization and when $\partial/\partial\varphi \neq 0$, and hence, the meta-atom is generally open to electromagnetic waves.

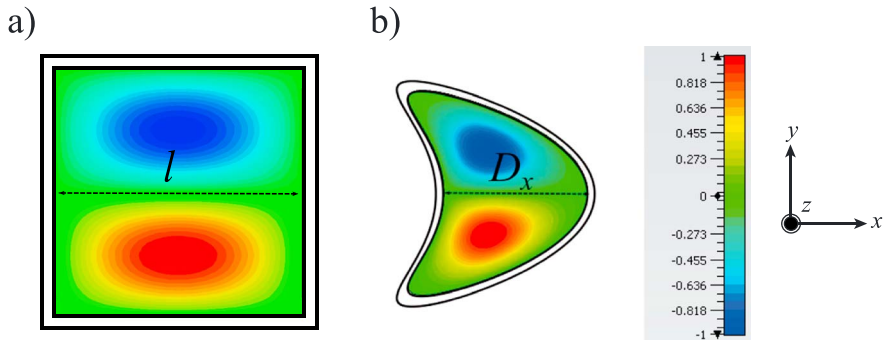

Figure 3. Snapshot in time of the magnetic field (H_z) associated with the dipolar trapped state (in arbitrary units) in a meta-atom with (a) a square-shaped and (b) a kite-shaped cross section, respectively. The corresponding electric field is on average directed along the *x* direction.

2.2. Other Geometries: Square-Shaped and Kite-Shaped Cross Sections

To demonstrate that the embedded eigenstates with infinite lifetime are not specific of meta-atoms with circular cross section, we studied the natural modes of open cavities with more complex shapes, such as a square- or a kite-shaped cross-section geometry (see Figure 3).

For a square-shaped cross-section geometry (Figure 3a), equation (2) has an analytical solution, $H_z = H_0 \sin\left(n\frac{\pi}{l}x\right)\sin\left(m\frac{\pi}{l}y\right)$, where $n, m = 1, 2, \ldots$ are integer numbers and l is the side of the square (it is supposed that the boundaries are $x = 0, l$ and $y = 0, l$). The associated eigenfrequencies are $\omega_{S,mn} = \frac{c}{\sqrt{\varepsilon_1}}\sqrt{\left(\frac{m\pi}{l}\right)^2 + \left(\frac{n\pi}{l}\right)^2}$.

Similar to the cylindrical case, the mode of interest cannot have a monopole-type symmetry. Indeed, the monopole mode $m = n = 1$ does not satisfy condition (2c) and hence must be excluded. For a dipolar-type symmetry, there are two options, $(m, n) = (1, 2)$ or $(m, n) = (2, 1)$, which correspond to $\omega_{S,12} = \frac{c}{\sqrt{\varepsilon_1}}\frac{\pi}{l}\sqrt{5}$. The profile of the relevant dipolar mode is depicted in Figure 3a. In order to have an embedded dipolar state, it is required that the plasma frequency of the ENZ material satisfies $\omega_p = \omega_{S,12}$ or equivalently the side of the square is equal to $l = \frac{c}{\sqrt{\varepsilon_1}}\frac{\pi}{\omega_p}\sqrt{5}$.

Evidently, for a completely generic geometry, for example, for a kite-shaped cross section (see Figure 3b), equation (2) does not have an analytical solution. In this case, the allowed oscillation frequencies of the embedded eigenstates need to be numerically determined. We used a commercial electromagnetic simulator (CST, 2016) to calculate the resonant frequencies of the equivalent cavity with PMC walls. The profile of lowest frequency dipolar mode (the dipolar modes are nondegenerate for this geometry) is represented in Figure 3b. From the numerical simulation, it is found that the resonant frequency is related to the diameter of the object D_x (along the *x* direction) as $\omega_K = \frac{6.41c}{D_x\sqrt{\varepsilon_1}}$, so that the light trapping condition is $D_x = \frac{6.41c}{\omega_p\sqrt{\varepsilon_1}}$. In summary, the geometrical conditions required to have infinite-lifetime oscillations with a dipolar mode in each of the meta-atom geometries are as follows:

$$\begin{aligned} R_{1,0} &= \frac{3.83c}{\omega_p\sqrt{\varepsilon_1}}\ , \quad \text{circular-shaped} \\ l_0 &= \frac{\sqrt{5}\pi c}{\omega_p\sqrt{\varepsilon_1}}\ , \quad \text{square-shaped}\ . \\ D_{x,0} &= \frac{6.41c}{\omega_p\sqrt{\varepsilon_1}}\ , \quad \text{kite-shaped} \end{aligned} \tag{9}$$

Note that in the ideal case wherein the ENZ shell is lossless, the light trapping condition is totally independent of the geometry of the shell (Liberal, Mahmoud, & Engheta, 2016; Liberal & Engheta, 2016a, 2016b; Silveirinha, 2014).

3. Meta-atom Excitation in the Linear Regime

Up to now, the discussion was focused on the physical nature and properties of the embedded eigenstates. Next, we analyze the electromagnetic response of a meta-atom under external excitation.

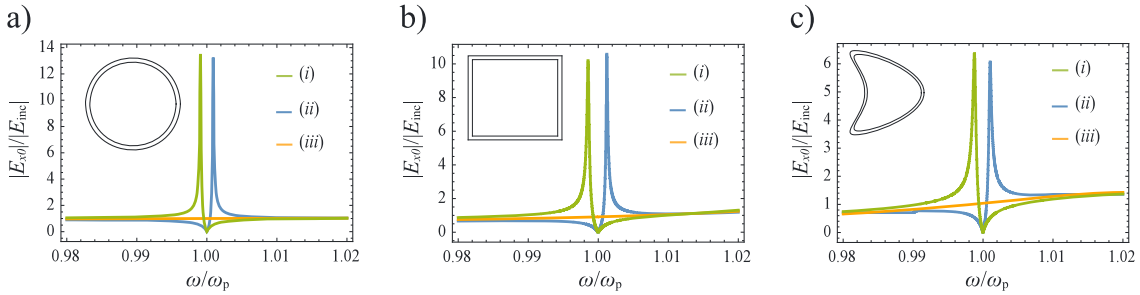

Figure 4. Normalized electric field in the meta-atom geometrical center as a function of the frequency for the (a) circular geometry, (b) square geometry, and (c) kite geometry. The curves (*iii*) correspond to meta-atoms that support embedded dipolar-type eigenstates with infinite lifetime, that is, for which condition (9) is satisfied. The curves (*i*) and (*ii*) correspond to objects with linear dimensions scaled by a factor of (*i*) 1.02 and (*ii*) 0.98 as compared to the tuned geometry (curve (*iii*)). The effect of ENZ loss is neglected in the simulation ($\omega_c/\omega_p \approx 0$). The inner core has permittivity $\varepsilon_1 = 1$ for the circular-geometry and $\varepsilon_1 = 2$ for the square and kite geometries.

The meta-atom is illuminated by a linearly polarized plane wave with magnetic field along the *z* direction and electric field along the *x* direction. Figure 4 depicts the ratio between the electric field in the meta-atom core center (E_{x0}) and the incident electric field amplitude (E_{inc}) as a function of the frequency for the three geometries introduced in section 2. The results of Figure 4 were obtained using CST Microwave Studio (CST, 2016). Note that E_{x0}/E_{inc} may be regarded as the transfer function of the meta-atom. For the circular cross-section case, E_{x0}/E_{inc} can be determined as well using Mie theory (for cylindrical waves), (Silveirinha, 2014) and is given by the Mie coefficient a_1^{TM} of the inner core.

For each cross-sectional shape, we consider three different resonators with linear dimensions scaled by a factor of (*i*) 1.02, (*ii*) 0.98, and (*iii*) 1.00 relative to the ideal geometry (equation (9)) for which the meta-atom supports an embedded dipolar-type state with infinite lifetime. As seen in Figure 4, independently of the cross section, all the meta-atoms exhibit a similar response to the plane-wave excitation. In particular, when the meta-atom dimensions are slightly detuned from the optimum value in equation (9) (curves (*i*) and (*ii*)), the scattering coefficients display resonances with Fano-type lineshapes (Luk'yanchuk et al., 2010), similar to the spherical geometry case (Silveirinha, 2014). The fractional bandwidth of the resonance is inversely proportional to the quality factor, and hence for a perfectly tuned meta-atom (curves (*iii*)), the transfer function does not have resonant features and $|E_{x0}/E_{inc}| \approx 1$ (Silveirinha, 2014). Hence, counterintuitively, in the tuned case the meta-atom is penetrable by the incoming radiation, which further highlights that the considered cavity is open to external excitations.

To shed some light on this intriguing property, the time dynamics of the electric field inside the meta-atom with circular cross section was studied with CST Microwave Studio (CST, 2016). The nanostructure is illuminated by a linearly polarized plane wave with finite duration in time (Gaussian-shaped pulse). The wave propagates along the positive *y* direction, and the Gaussian pulse is centered at $t_{peak} = 177$ ps with a full-width half maximum equal to $\Delta\tau = 78$ ps. The plasma frequency of the ENZ material is $\omega_p/(2\pi) = 1$ THz, and the meta-atom radius is tuned according to equation (9).

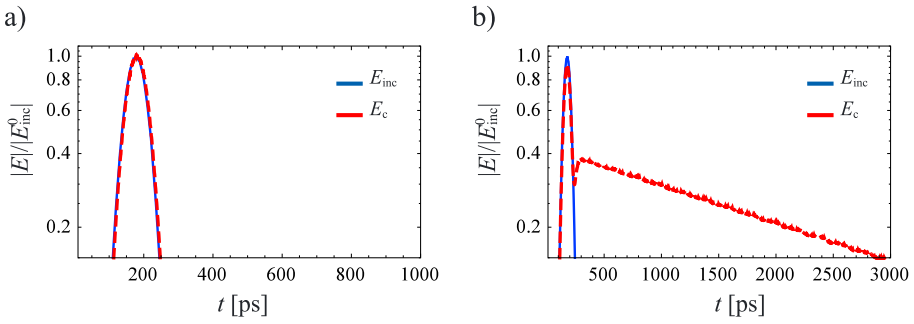

Figure 5. Time evolution of the electric field envelope at the center of the meta-atom for an incident pulse with a peak amplitude $|E^0_{inc}|$ for (a) $R_1 = R_{1,0}$ and (b) $R_1 = 0.98R_{1,0}$. The effect of ENZ loss is neglected in the simulation ($\omega_c/\omega_p \approx 0$); the inner core has relative permittivity $\varepsilon_1 = 1$ and $R_2 = 1.1R_1$.

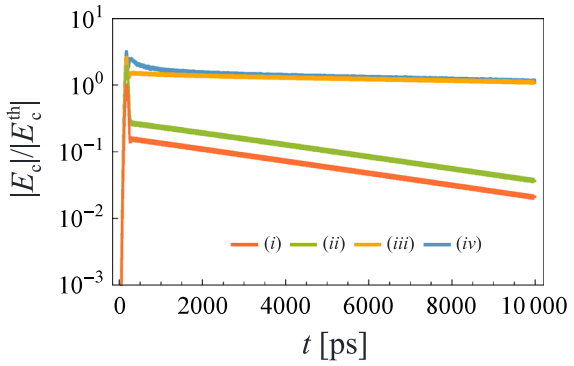

Figure 6. Time variation of the normalized electric field $|E_c|/|E_c^{th}|$ in the core for an excitation pulse with (*i*) $|E_{inc}^0| = 1|E_c^{th}|$, (*ii*) $|E_{inc}^0| = 2|E_c^{th}|$, (*iii*) $|E_{inc}^0| = 3|E_c^{th}|$, and (*iv*) $|E_{inc}^0| = 4|E_c^{th}|$, with the parameter $\chi^{(3)}$ fixed.

Figure 5a shows the normalized amplitude of the electric field at the center of the meta-atom as a function of time for a tuned cavity ($R_1 = R_{1,0}$). As seen, the electric field in the core is virtually coincident with the incoming field. This property is consistent with the fact that $|E_{x0}/E_{inc}| \approx 1$ (Figure 4a, *iii*); that is, a perfectly tuned meta-atom is nearly transparent to the incoming radiation. Crucially, this property implies that the external excitation is unable to pump the embedded eigenstate with infinite lifetime when $R_1 = R_{1,0}$. Thus, consistent with the Lorentz reciprocity theorem, in the same way as the light trapped in the embedded state cannot escape from the meta-atom, an external source is also unable to excite the embedded light state with infinite lifetime (Lannebère & Silveirinha, 2015; Silveirinha, 2014). In contrast, Figure 5b shows that when the structure is slightly detuned ($R_1 = 0.98R_{1,0}$), a significant part of the energy of the incoming field can remain trapped in the meta-atom and relax slowly with a decay rate $\omega'' = 4.12 \times 10^8$ rad/s, long after the incident pulse overtakes the meta-atom.

4. Meta-atom Excitation in the Nonlinear Regime: Trapping a Light "Bit"

In Lannebère and Silveirinha (2015), it was shown that the limitations imposed by the Lorentz reciprocity theorem can be surpassed with the help of a nonlinear response. The key idea is to use a nonlinear material in the core region and choose the core dimensions slightly below the optimum. The slight detuning of the inner core allows the relevant eigenstate to be externally pumped (Figure 5b), whereas the nonlinear material enables the resonator self-tuning and the trapping of a quantized amount of light energy (Lannebère & Silveirinha, 2015). Here we will explore the same mechanism but for complex-shaped 2D meta-atoms.

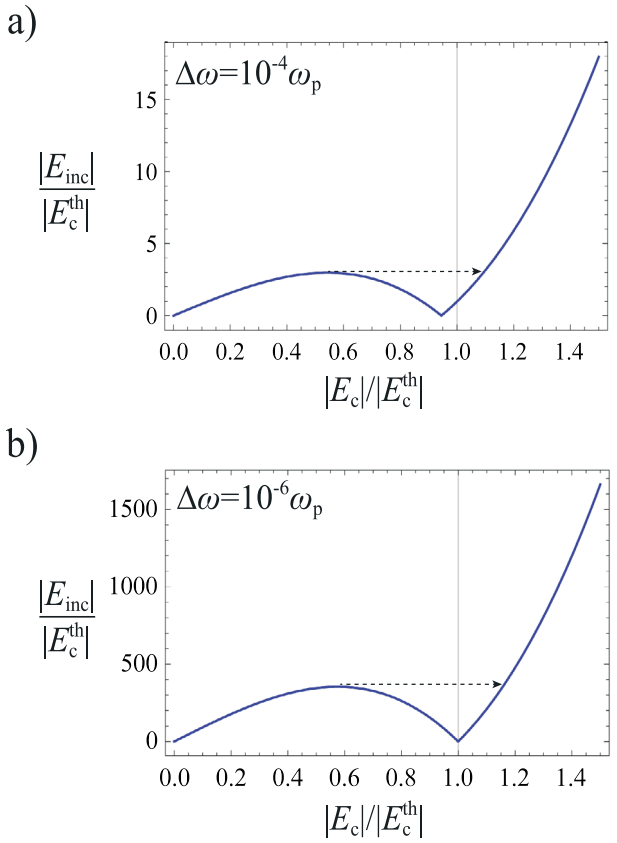

Figure 7. Bistable characteristic of the meta-atom for the fixed frequency $\omega = \omega_p + \Delta\omega$ with (a) $\Delta\omega = 10^{-4}\omega_p$ and (b) $\Delta\omega = 10^{-6}\omega_p$. The arrow indicates the discontinuous transition between different branches.

To begin with, we consider a meta-atom with a circular cross section and set the inner radius equal to $R_1 = 0.98R_{1,0}$. Assuming that the core has a Kerr-type nonlinear response, the condition to obtain a perfect trapping at the frequency ω_p can be estimated as $k_1^{NL}R_1 = k_1R_{1,0}$ (Lannebère & Silveirinha, 2015), where $k_1^{NL} = \sqrt{\varepsilon^{NL}}\frac{\omega_p}{c}$ is the wavenumber inside the nonlinear medium and ε^{NL} is the relative nonlinear permittivity. This condition is equivalent to (Lannebère & Silveirinha, 2015)

$$\chi^{(3)}\frac{3}{4}|E_c|^2 = \varepsilon_1\left[\left(\frac{R_{1,0}}{R_1}\right)^2 - 1\right], \tag{10}$$

where $\chi^{(3)}$ is the third-order susceptibility of the nonlinear material (Boyd, 2008) and E_c is the electrical field complex amplitude at the core center in the stationary state. A similar condition holds for the other cross-section geometries considered in this article with $R_{1,0}/R$ replaced by l_0/l for the square-shaped meta-atom and by $D_{x,0}/D_x$ for the kite-shaped meta-atom. Importantly, equation (10) reveals that E_c, and thereby also the field energy trapped in the meta-atom, are precisely quantized and only depend on the geometrical parameters of the resonator and on the considered materials.

To demonstrate these ideas, we studied the time dynamics of the electric field in the open resonator when it is excited by a pulse with the same Gaussian profile as in the previous section. As discussed in Lannebère and Silveirinha (2015), the effect of loss in the ENZ material is strongly detrimental to the light trapping in the core (see Figure 2), and in practice, the ENZ material loss needs to be compensated by

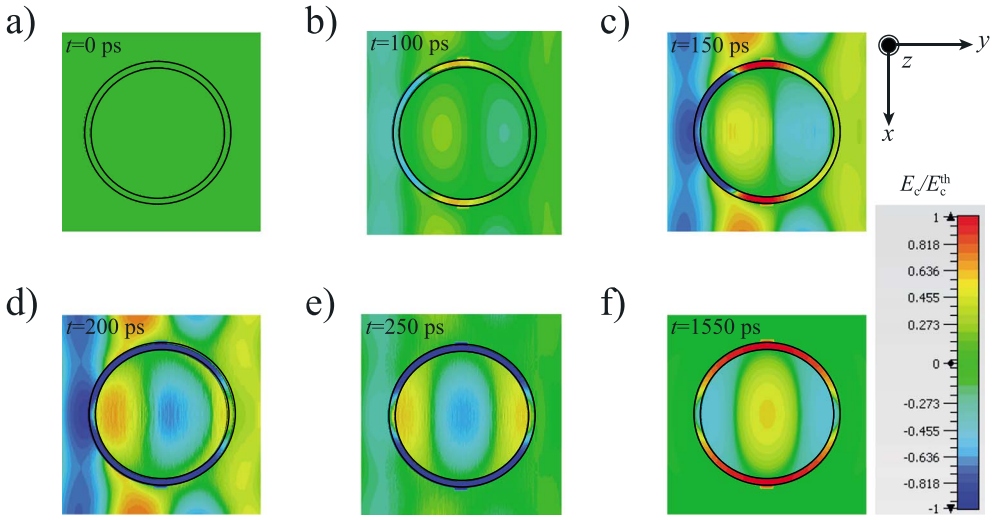

Figure 8. Time snapshots of the *x* component of the electric field in the *xoy* plane showing the excitation of the meta-atom by the incoming pulse that propagates along the +*y* direction, and the trapping of a light "bit" in the core after the incoming pulse overtakes the meta-atom.

some active material with optical gain. Thus, in what follows, it is assumed that the ENZ shell is lossless ($\omega_c/\omega_p \approx 0$).

Figure 6 depicts the peak amplitude of the electric field in the core (i.e., the field envelope) as a function of time for different values of the peak amplitude of the incident field $|E^0_{inc}|$. For the sake of generality, we use normalized units so that the electric field is normalized to $|E^{th}_c| = \sqrt{\frac{4\varepsilon_1}{3\chi^{(3)}}\left[\left(\frac{R_{1,0}}{R_1}\right)^2 - 1\right]}$, that is, the theoretical value of the field in steady-state regime (equation (10)). For example, if the third-order nonlinear susceptibility of the core is $\chi^{(3)} = 10^{-18}\ m^{-2}V^{-2}$ and $\varepsilon_1 = 1$, one has $|E^{th}_c| = 2.3\times10^8\,V/m$.

The results of Figure 6 confirm that in the stationary regime E_c always saturates at the same value (curves (*iii*) and (*iv*)), and hence, the trapped light energy is indeed quantized. In our example, the saturation value is $|E_c| = 1.16|E^{th}_c|$, showing that theoretical formula (10) underestimates the field in the core. The difference is expected because equation (10) is derived under the assumption that the electric field is uniform in the core. Thus, in steady state the required nonlinearity strength is $\chi^{(3)}|E_c|^2 = 0.07$. The nonlinearity strength can be made as small as one wishes with a design with $R_1/R_{1,0}$ closer to the unity. Moreover, one can see from Figure 6 that there is a threshold value for $|E^0_{inc}|$ and the light trapping only occurs for incident pulses with amplitude larger than the threshold. In the example of Figure 6, the threshold is roughly $|E^0_{inc}| = 3|E^{th}_c|$ (curve (*iii*)).

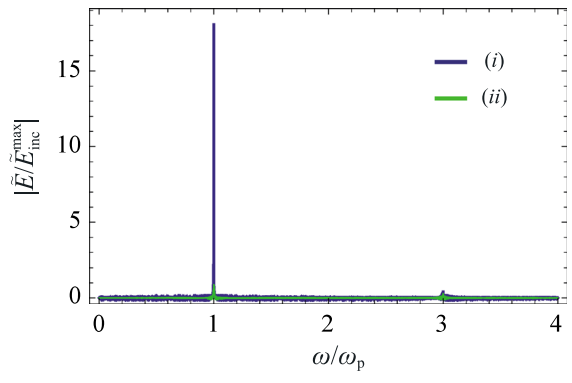

Figure 9. Plot of the Fourier transform of the *x* component of the electric field normalized to the peak value of the Fourier transform of the incident wave: (*i*) at the center of the meta-atom and (*ii*) outside the meta-atom, at $(x, y, z) = (0, 1.5R_2, 0)$. The duration of the simulation is $114\Delta\tau$, and the simulation parameters are as in Figure 6 (*iii*).

To further understand the nonlinear mechanisms that enable the light trapping, we show in Figure 7 the normalized field in the core (in the horizontal axis) as a function of the normalized incident field (in the vertical axis) in the nonlinear regime and for two fixed frequencies near ω_p. This plot was obtained using $|E_{inc}| = \frac{1}{|a_1^{TM}|}|E_c|$, with a_1^{TM} the Mie coefficient in the core. The Mie coefficient is a function of the core permittivity $\varepsilon^{NL} = \varepsilon_1 + \frac{3}{4}\chi^{(3)}|E_c|^2$ and thereby of the core electric field. Remarkably, the characteristic $|E_c|$ versus $|E_{inc}|$ is multivalued, and hence, the meta-atom has a bistable response.

The light trapping occurs at the point $|E_c| = |E^{th}_c|$ and $|E_{inc}| = 0$ when $\omega = \omega_p$. To reach this point, the amplitude of the incoming wave must exceed a threshold value, so that the transition between the two

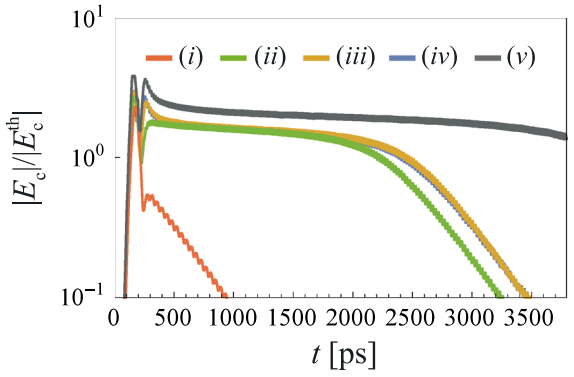

Figure 10. (a) Time variation of the normalized electric field at the center of the kite-shaped meta-atom for an incident pulse with peak amplitudes (*i*) $|E^0_{inc}| = 3|E^{th}_c|$, (*ii*) $|E^0_{inc}| = 4|E^{th}_c|$, (*iii*) $|E^0_{inc}| = 5|E^{th}_c|$, and (*iv*) $|E^0_{inc}| = 6|E^{th}_c|$. Curve (*v*) is for a kite with diameter $D_x = 0.99D_{x,0}$ and an incident pulse with peak amplitude $|E^0_{inc}| = 7.13|E^{th}_c|$.

branches (indicated by the arrow) may take place. This threshold value depends strongly on the frequency detuning $\Delta\omega$ with respect to $\omega = \omega_p$. The threshold value is roughly $3|E^{th}_c|$ for curve (a) and $350|E^{th}_c|$ for curve (b) and approaches infinity in the limit $\Delta\omega \to 0$. In practice, the meta-atom is excited by a finite duration pulse with a spectrum sufficiently wide to excite a continuum range of $\Delta\omega$. Thus, the threshold value that enables the transition from the first to the second branch is determined by the global frequency response of the meta-atom.

To illustrate the dynamics of the light trapping, we show in Figure 8 several time snapshots of the *x* component of the electric field for the simulation of Figure 6 (*iii*). Figure 8 clearly shows that a quantized amount of the energy of the excitation pulse stays trapped in the open resonator and that there is no energy leaked to the exterior after the core permittivity is self-tuned.

As a result of the nonlinear response of the dielectric core, there is a frequency conversion so that a third-order harmonic is generated in the core (see Figure 9). The third-order harmonic generation may affect the mode lifetime and may contribute to the relaxation of the trapped light (Lannebère & Silveirinha, 2015), but the process appears to be rather slow.

In order to investigate the impact of changing the cross-section geometry, we also analyzed the temporal dynamics of the fields in a kite-type resonator (see Figure 3b). Figure 10 shows the normalized electric field peak amplitude at the center of the kite-shaped meta-atom for different amplitudes of the incident pulse. The diameter of the kite-shaped object is $D_x = 0.98D_{x,0}$ (curves (*i*–*iv*)), and the core permittivity in the linear regime is $\varepsilon_1 = 2$. The excitation pulse and the ENZ material are the same as in the previous examples. The results of Figure 10 are somewhat analogous to those of the circular cross-section case in Figure 6. In particular, in the trapping regime the field in the core has a nearly constant amplitude. However, the kite geometry appears to be much more sensitive to realistic decay mechanisms (e.g., third harmonic conversion or absorption effects), because after the time instant $t = 2000$ ps the light bit escapes from the core at the same rate as in the linear regime. This increased sensitivity to relaxation mechanisms as compared to the meta-atom with circular cross section is in part due to the lower quality factor of the kite resonator (see Figure 4). In fact, for a kite resonator with a larger quality factor ($D_x = 0.99D_{x,0}$; curve (*v*) of Figure 10), the light bit is withheld in the core for a considerably longer period of time. However, it is evident that the circular cross-section geometry enables a more robust performance.

5. Conclusion

It was demonstrated that the light trapping mechanism introduced in Lannebère and Silveirinha (2015) and Silveirinha (2014) may be generalized to open core-shell plasmonic particles with arbitrary shape. When some particular geometrical conditions are satisfied, complex-shaped cavities can support embedded eigenstates that in the lossless limit have an infinite lifetime. Moreover, it was shown that a fundamental restriction imposed by the Lorentz reciprocity theorem, which forbids the direct external excitation of the embedded eigenstates, can be circumvented with a nonlinear dielectric response, similar to what was done in Lannebère and Silveirinha (2015) for a spherical core-shell geometry. The amount of energy retained within the meta-atom is precisely quantized and depends only on the core-shell geometry. The numerical simulations suggest that the meta-atom geometry has a considerable influence on the sensitivity to relaxation mechanisms.

Acknowledgments
This work is supported in part by Fundação para a Ciência e a Tecnologia grants PTDC/EEITEL/4543/2014 and UID/EEA/50008/2013 and by the Instituto de Telecomunicações under project C00355-TRAP. Solange Silva and Tiago Morgado gratefully acknowledge support by Fundação para a Ciência e a Tecnologia, under the fellowships SFRH/BD/105625/2015 and SFRH/BPD/84467/2012. This paper is theoretical and thus does not include new data or modeling.

References

Alù, A., Silveirinha, M. G., Salandrino, A., & Engheta, N. (2007). Epsilon-near-zero metamaterials and electromagnetic sources: Tailoring the radiation phase pattern. *Physical Review B*, *75*(15), 155410. https://doi.org/10.1103/PhysRevB.75.155410
Boyd, R. W. (2008). *Nonlinear optics* (3rd ed.). New York: Academic Press.

Capasso, F., Sirtori, C., Faist, J., Sivco, D. L., Chu, S.-N. G., & Cho, A. Y. (1992). Observation of an electronic bound state above a potential well. *Nature*, *358*, 565. https://doi.org/10.1038/358565a0

CST GmbH 2016 CST microwave studio. Retrieved from http://www.cst.com

Engheta, N. (2013). Pursuing near-zero response. *Science*, *340*(6130), 286–287. https://doi.org/10.1126/science.1235589

Hrebikova, I., Jelinek, L., & Silveirinha, M. G. (2015). Embedded energy state in an open semiconductor heterostructure, *Physical Review B*, *92*(15), 155303. https://doi.org/10.1103/PhysRevB.92.155303

Hsu, C. W., Zhen, B., Lee, J., Chua, S.-L., Johnson, S. G., Joannopoulos, J. D., & Soljačić, M. (2013). Observation of trapped light within the radiation continuum. *Nature*, *499*(7457), 188–191. https://doi.org/10.1038/nature12289

Hsu, C. W., Zhen, B., Stone, A. D., Joannopoulos, J. D., & Soljačić, M. (2016). Bound states in the continuum. *Nature Reviews Materials*, *1*(9), 16048. https://doi.org/10.1038/natrevmats.2016.48

Lannebère, S., & Silveirinha, M. G. (2015). Optical meta-atom for localization of light with quantized energy. *Nature Communications*, *6*, 8766. https://doi.org/10.1038/ncomms9766

Lee, J., Zhen, B., Chua, S.-L., Qiu, W., Joannopoulos, J. D., Soljačić, M., & Shapira, O. (2012). Observation and differentiation of unique high-Q optical resonances near zero wave vector in macroscopic photonic crystal slabs. *Physical Review Letters*, *109*(6), 067401. https://doi.org/10.1103/PhysRevLett.109.067401

Liberal, I., & Engheta, N. (2016a). Nonradiating and radiating modes excited by quantum emitters in open epsilon-near-zero cavities. *Science Advances*, *2*(10), e1600987. https://doi.org/10.1126/sciadv.1600987

Liberal, I., & Engheta, N. (2016b). Zero-index platforms: Where light defies geometry. *Optics & Photonics News*, *27*(7), 26–33. https://doi.org/10.1364/OPN.27.7.000026

Liberal, I., Mahmoud, A. M., & Engheta, N. (2016). Geometry-invariant resonant cavities. *Nature Communications*, *7*, 10989. https://doi.org/10.1038/ncomms10989

Luk'yanchuk, B., Zheludev, N. I., Maier, S. A., Halas, N. J., Nordlander, P., Giessen, H., & Chong, C. T. (2010). The Fano resonance in plasmonic nanostructures and metamaterials. *Nature Materials*, *9*(9), 707–715. https://doi.org/10.1038/nmat2810

Marinica, D. C., Borisov, A. G., & Shabanov, S. V. (2008). Bound states in the continuum in photonics. *Physical Review Letters*, *100*(18), 183902. https://doi.org/10.1103/PhysRevLett.100.183902

Molina, M. I., Miroshnichenko, A. E., & Kivshar, Y. S. (2012). Surface bound states in the continuum. *Physical Review Letters*, *108*(7), 070401. https://doi.org/10.1103/PhysRevLett.108.070401

Monticone, F., & Alù, A. (2014). Embedded photonic eigenvalues in 3D nanostructures. *Physical Review Letters*, *112*(21), 213903. https://doi.org/10.1103/PhysRevLett.112.213903

Plotnik, Y., Peleg, O., Dreisow, F., Heinrich, M., Nolte, S., Szameit, A., & Segev, M. (2011). Experimental observation of optical bound states in the continuum. *Physical Review Letters*, *107*(18), 183901. https://doi.org/10.1103/PhysRevLett.107.183901

Silveirinha, M. G. (2014). Trapping light in open plasmonic nanostructures. *Physical Review A*, *89*(2), 023813. https://doi.org/10.1103/PhysRevA.89.023813

Silveirinha, M. G., & Engheta, N. (2006). Tunneling of electromagnetic through subwavelength channels and bends using ε-near-zero materials. *Physical Review Letters*, *97*(15), 157403. https://doi.org/10.1103/PhysRevLett.97.157403

Silveirinha, M. G., & Engheta, N. (2009). Transporting an image through a subwavelength hole. *Physical Review Letters*, *102*(10), 103902. https://doi.org/10.1103/PhysRevLett.102.103902

Stillinger, F. H., & Herrick, D. R. (1975). Bound states in the continuum. *Physical Review A*, *11*(2), 446–454. https://doi.org/10.1103/PhysRevA.11.446

von Neumann, J., & Wigner, E. (1929). Über merkwürdige diskrete eigenwerte. *Physikalishce Zeitschrift*, *30*, 465. https://doi.org/10.1007/978-3-662-02781-3_19